International Journal of Rotating Machinery
1996, Vol. 2, No. 3, pp. 149-159
Reprints available directly from the publisher
Photocopying permitted by license only

Impeller Flow Field Laser Velocimeter Measurements

L. A. BROZOWSKI, T. V. FERGUSON and L. ROJAS
Rockwell International Corporation, Rocketdyne Division, Canoga Park, California

(Received August 9, 1995)

Development of Computational Fluid Dynamics (CFD) computer codes for complex turbomachinery affords a complete three-dimensional (3-D) flow field description. While significant improvements in CFD have been made due to improvements in computers, numerical algorithms, and physical modeling, a limited experimental database for pump CFD code validation exists.

Under contract (NAS8-38864) to the National Aeronautics and Space Administration (NASA) at Marshall Space Flight Center (MSFC) a test program was undertaken at Rocketdyne to obtain benchmark data for typical rocket engine pump geometry. Nonintrusive velocity data were obtained with a laser two-focus velocimeter. Extensive laser surveys at the inlet and discharge of a Rocketdyne-designed impeller were performed. Static pressures were measured at key locations to provide boundary conditions for CFD code validation.

Key Words: *Impeller flow; two-dimensional; laser velocimeter*

INTRODUCTION

Development of Computational Fluid Dynamics (CFD) computer codes for complex turbomachinery affords three-dimensional (3-D) flow field calculations. However, existing data for pump CFD code validation is limited. Accurate databases are required to validate the CFD codes to enable evaluation of existing turbulence models and grid number requirements.

Traditional flow field survey information from pressure sensors and directional probes are intrusive and typically yield an uncertainty in excess of 0.5% of full range and thus do not yield quality benchmark data. Pressure sensors and directional probes only yield circumferentially averaged information. Laser velocimetry is nonintrusive and yields accurate flow velocity and angle data. More importantly, laser velocimetry provides information at specific circumferential locations blade to blade.

The objective of the test program undertaken was to obtain benchmark quality data, flow velocity and angle at key locations in a generic pump operating at the impeller design flow rate. These data along with data from a similarly tested impeller [1, 2] will be used by the Consortium for Computational Fluid Dynamics Application in Propulsion Technology Pump Stage Team [3] to validate pump CFD codes.

The tested configuration consisted of a four-bladed unshrouded inducer, a shrouded impeller with six full blades and six partial blades, in conjunction with a diffusing crossover and discharge plenum. The flow field survey consisted of 10 radial stations along one axial plane at the impeller inlet, 11 axial stations in a radial plane immediately downstream of the impeller discharge, and 9 axial stations close to the crossover inlet. The fluid medium for the laser velocimeter surveys was ambient water.

Data are nondimensionalized as follows:

Nondimensional Length:

$$L_{nondim} = \frac{L}{D_{tip}} \quad (1)$$

where:

L is length

D_{tip} impeller tip diameter

Nondimensional Head:

$$H_{nondim} = \frac{g_c H}{U_{tip}^2} \quad (2)$$

where:

H is head

g_c is the gravitational constant

U_{tip} is the impeller discharge tip speed
Nondimensional Velocity:

$$V_{nondim} = \frac{V}{U_{tip}} \qquad (3)$$

where:
V is velocity
U_{tip} is the impeller discharge tip speed

TEST ARTICLE

The test article was a Rocketdyne-designed shrouded impeller that met the operational requirements for the Space Transportation Main Engine (STME) fuel pump and designated the "Consortium baseline impeller." Table 1 summarizes the impeller geometry and test conditions. Figure 1 provides a layout of the impeller blades.

The impeller was tested with an axial inlet and a four-bladed unshrouded inducer. The axial spacing between the inducer and impeller was intended to minimize the inducer wake effects at the impeller inlet while still providing enough critical speed margin for rotordynamic stability. Testing the impeller in conjunction with an axial inlet and inducer provided geometry typical of current rocket engine pumps.

While the test article geometry reflected current rocket engine designs, the impeller shroud wear ring clearance was purposely atypical of an engine. The nondimensional radial clearance between impeller shroud and the polypropylene seal was nominally −0.000166. The radial interference fit minimized impeller discharge recirculation flow that may be more useful for validation of current CFD codes. This arrangement affords less complex CFD modeling since both the front and rear shroud recirculation zones can be eliminated.

The test configuration, presented in Figure 2, included a crossover discharge to minimize asymmetric flow at the impeller discharge.

TEST FACILITY

The test program was conducted in the Engineering Development Laboratory (EDL) Pump Test Facility (PTF) located at Rocketdyne's main facility in Canoga Park, California. A schematic of the flow loop is presented in Figure 3. The test article was driven by a 1,200-rpm, reversible, synchronous electric motor rated at 2,984 kW. The motor was coupled to a 2,984-kW gearbox capable of producing speeds of 6,322, 8,013, and 10,029 rpm. The pump CFD code validation configuration was tested at 6,322 rpm.

Water was supplied to the closed flow loop from a 28.769-m^3 stainless steel tank. The tank was rated at 1.0342 MPa with a vacuum capability of 0.0962 MPa. A heat exchanger located adjacent to the tank maintained a uniform fluid inlet temperature. The flow rate to the tester was regulated by a throttle valve downstream of the pump. After passing through the throttle valve and into the tank, the flow passed through a series of baffles in the tank and was recirculated through the facility.

TEST INSTRUMENTATION

Two four-tap static piezometer rings were used to measure the inlet static pressure. They were located approximately 13.5 and 8.7 inlet pipe diameters upstream of the inducer. Water temperature was measured in the inlet line with a platinum wire filament temperature detector to allow calculation of the fluid density and vapor pressure.

Three impeller inlet static pressure measurements were aligned in one axial plane, but distributed around

TABLE 1
Design details of test article

Parameter	Value
Number of impeller full blades	6
Number of impeller partial blades	6
Nondimensional inlet eye diameter	0.6633
Shaft speed (rpm)	6,322
Impeller tip speed (m/s)	76.0493
Nondimensional impeller shroud wear ringradial clearance	−0.000166
Impeller inlet design flow coefficient*	0.144
Nondimensional inducer tip radial clearance	0.000967
Nondimensional impeller B_2 width	0.078699
Nondimensional impeller shroud thickness at discharge	0.01393
Nondimensional impeller hub thickness at discharge	0.01739

*Based on tester inlet flow and impeller eye speed. Does not take recirculation flow into account

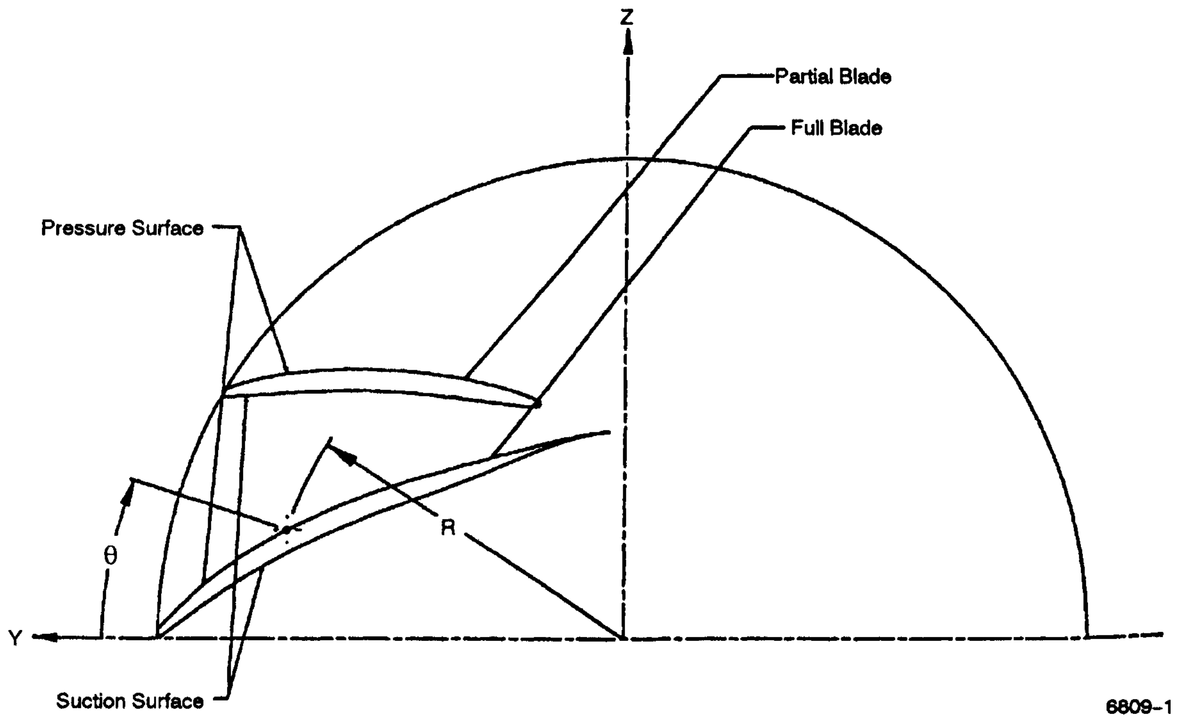

FIGURE 1 Impeller blade layout.

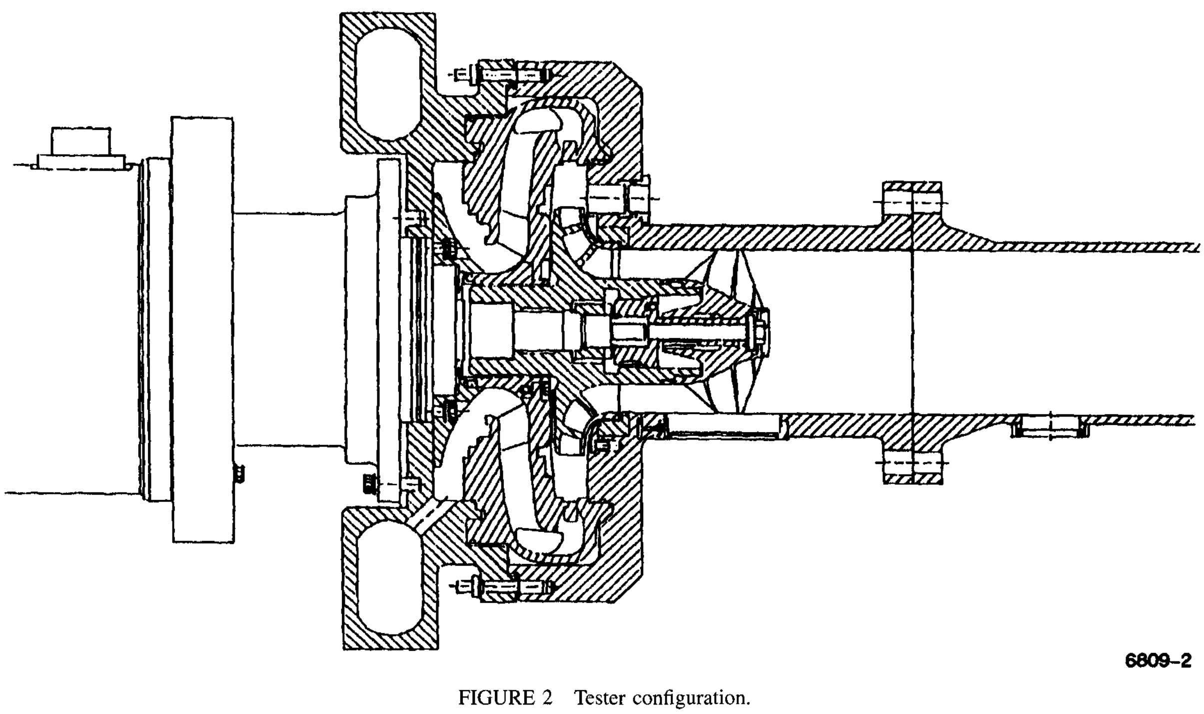

FIGURE 2 Tester configuration.

the circumference (90 deg apart) to identify any circumferential pressure variations of impeller inlet flow. This identification is important because the impeller inlet laser survey occurs at one particular circumferential location. Circumferential variations are not reflected in the laser survey. The impeller inlet static pressure tap plane was located a nondimensional axial length of 0.0766 downstream of the laser survey plane.

Similarly, identification of circumferential variations at the impeller discharge was accommodated by three static pressure taps located around the tester circumference in a plane midway between the two impeller discharge laser survey planes. One static pressure tap was included at each of the two laser survey radial planes. A differential static pressure measurement between the lowest radial impeller discharge survey plane and the tester inlet provided redundancy. All pressure measurements were obtained with Taber full bridge strain gage transducers with an accuracy of $\pm$ 0.5% of full range. Flow rate was measured with one 20.32-cm turbine-type flowmeter in the inlet line with measurement redundancy provided by another 20.32-cm turbine-type flowmeter in the discharge line. Additional instrumentation was employed for facility monitoring and computer redlines.

TEST PROGRAM

The test program comprised a fiber-optic laser two-focus (L2F) velocimeter survey in one axial plane at the impeller inlet and two radial surveys at the impeller discharge. Table 2 lists the nondimensional radial positions of the impeller inlet survey referenced from the shaft centerline. The positions are also identified in terms of the percentage of the laser survey plane annulus height. With this designation, 0% is the hub and 100% is the laser window face on the inner diameter of the inlet housing. The nondimensional axial length between the laser survey plane and the impeller leading edge tip was -0.1290. The negative sign indicates an axial location upstream of the axial reference zero. The laser velocimeter is capable of partitioning any given circumferential section into 16 separate data zones called "windows." For the tested configuration inlet survey, data were acquired over two adjacent 90-deg segments. The survey was performed over 180 circumferential degrees because the inducer had four blades and the impeller had six full blades; it was not known a priori if inducer or impeller effects would dominate the flow field at the survey location. With 16 windows, data were segregated into distinct flow zones of 5.625-deg (90 deg/16 windows) angular sweep. An axial projection of a blade leading-edge tip intersection with the impeller shroud was used as the centerline of an impeller inlet timing mark which was machined into the impeller hub. This mark allowed triggering the start of the laser survey to be coincident with an impeller full blade. The center of the timing mark was used to commence circumferential laser velocimeter surveys at all annulus heights. Since adjacent 90-deg survey arcs were not similar in terms of impeller blade location, data were not ensemble averaged.

The impeller discharge surveys were performed at multiple axial locations along two radial planes. The nondimensional radial locations of the axial surveys were 0.5138 and 0.5597. The plane located at a nondimensional radius of 0.5138 was immediately downstream of the impeller discharge. The plane located at a nondimensional radius of 0.5597 was the furthest downstream survey possible and at an approximate location of downstream components in actual hardware. Table 3 lists the laser survey nondimensional axial positions referenced from the impeller discharge tip shroud, 0.0% of impeller B_2 width. A negative value occurs when the axial location of the survey point is forward (toward the tester inlet) of the impeller discharge tip shroud. A value greater than 100% is indicative of a laser survey position at an axial distance toward the tester aft end, in excess of the impeller B_2 width.

Encompassed in a 60-deg segment between two adjacent full blades at the impeller discharge is a partial blade. Circumferential partitioning over two adjacent 30-deg segments provided better circumferential flow definition between adjacent blades. With 16 windows, data were segregated into distinct flow zones of 1.875 deg (30 deg/16 windows) of angular sweep. The impeller discharge timing mark centerline was located from an axial projection midway between the impeller suction and pressure surfaces at the impeller tip, 0% impeller B_2 width.

The center of the timing mark was used to commence circumferential laser velocimeter surveys at all axial survey locations. Adjacent 30-deg segments were not similar and ensemble averaging of the impeller discharge data was not performed.

Although the impeller inlet and discharge laser surveys spanned multiple test days and long time durations, a statistical analysis indicated that test-to-test parameter variations were negligible.

The tester shaft was marked and served to trigger the start of the laser velocimeter survey in the circumferential direction. This shaft mark was not necessarily coincident with the circumferential location of the timing mark machined at the inlet and discharge of the impeller. Therefore, the angular distance or equivalent time delay between the desired survey start and the laser start trigger

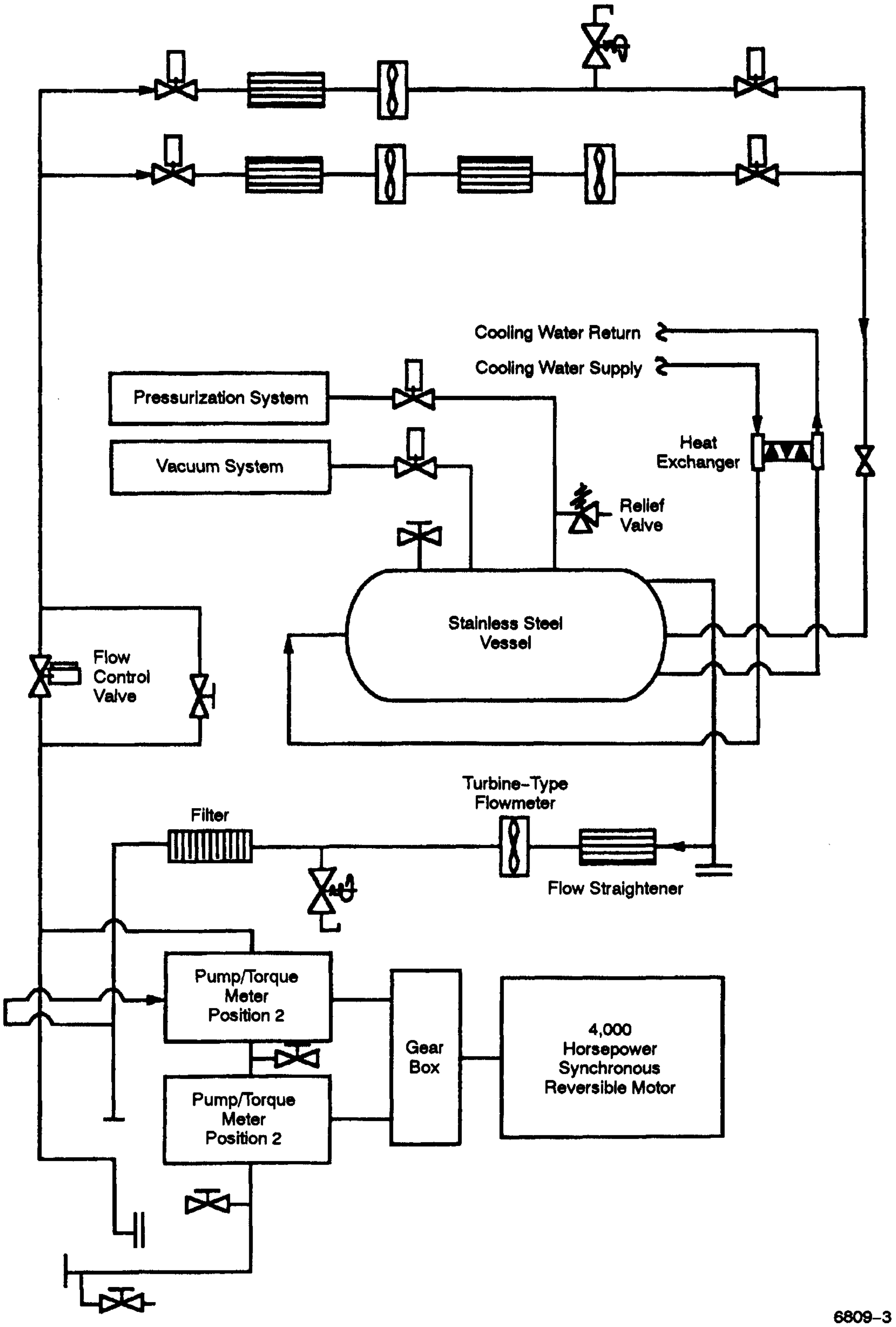

FIGURE 3 Engineering Development Laboratory Pump Test Facility-flow schematic.

TABLE 2
Impeller inlet laser survey radial locations

Nondimensional radius	Percent impeller inlet annulus height
0.22731	10
0.23317	15
0.24489	25
0.25660	35
0.26832	45
0.28004	55
0.29176	65
0.30348	75
0.31520	85
0.32692	95

were determined. A photonic sensor was used to generate a once-per-revolution (OPR) pulse from the drive shaft of the tester. A timing mark was machined onto the impeller surface as described in the section entitled Test Program. The L2F was positioned so that the measurement volumes were able to detect the timing mark and generate a scattered light signal. The light signal was converted to an electronic signal via the L2F signal processing electronics. The phase angle between the occurrence of the OPR pulse and the timing mark pulse was determined.

The phase angle between the OPR pulse and the impeller inlet timing mark signal was also performed as the assembly rotated at full speed. Good agreement existed between the static and dynamic phase angle methods at both the impeller inlet and discharge locations.

TEST RESULTS

The impeller inlet laser velocimeter survey, which may serve as a boundary condition to CFD codes, also serves as a check for data integrity. Laser surveys over 180 circumferential degrees (two inducer blade passages or three impeller blade passages) were performed because of the dissimilar number of inducer and impeller blades. Laser data indicated inducer effects were prevalent and no significant impeller effects were evident in the flow. Data integrity was checked with a flow continuity match, i.e., a comparison of integrated flow based on the laser velocimeter velocities to flow measured with two turbine-type flowmeters. A continuity match of 98.6% was achieved at design flow coefficient. Discrepancies between integrated and measured flow may occur because of grid coarseness and/or use of a trapezoid integration scheme that does not include interpolation of the flow velocity to the walls. The continuity match was consistent with those calculated during previous test programs.

TABLE 3
Impeller discharge laser survey axial locations

Nondimensional axial location from reference	Percent impeller B_2 width
Nondimensional radius = 0.5138	
0.15427	−32.6
0.16013	−25.1
0.18976	12.5
0.19960	25.0
0.20944	37.5
0.21927	50.0
0.22911	62.5
0.23895	75.0
0.24878	87.5
0.26391	106.7
0.27903	125.9
Nondimensional radius = 0.5597	
0.15427	−32.6
0.16013	−25.1
0.19304	16.7
0.20616	33.3
0.21927	50.0
0.23239	66.7
0.24551	83.3
0.26094	102.9
0.27638	122.6

Table 4 presents a summary of the impeller inlet flow characteristics for one of the 90-deg surveys. The average values at each radial position were essentially the same for both 90-deg circumferential surveys. The summary compiles nondimensional absolute velocity (C/U_{tip}), nondimensional absolute tangential velocity (Cu/U_{tip}), nondimensional absolute axial velocity (Ca/U_{tip}), absolute flow angle, nondimensional relative velocity (W/U_{tip}), nondimensional relative tangential velocity (Wu/U_{tip}), and relative flow angle at each radial position surveyed. The values presented reflect flow-weighted nondimensional velocity, flow-weighted nondimensional tangential velocity, and area-weighted axial velocity. The other values were derived from these parameters. Bulk flow quantities were derived over all radii and represent average values for the entire flow. The hub to tip distribution of axial velocity is linear over most of the flow annulus, between 25 and 90% of impeller inlet annulus. Figures 4 and 5 present contour plots of the impeller inlet axial and tangential velocity components. The relative tangential velocity, axial velocity, and incidence angle at the impeller inlet are the parameters that affect the impeller discharge flow characteristics and hydrodynamic performance.

No significant circumferential pressure variations were detected at the impeller inlet. The variations measured were within transducer accuracy.

At the impeller discharge, the flow continuity match, calculated across the data locations within the impeller

TABLE 4
Impeller inlet flow characteristics

NRA Pump CFD Code Validation Test
Laser Velocimeter surveys, ambient water, impeller inlet survey.
Test Number: t92a053,54,56 Test Date: October 1992 Impeller Inlet Data Set 1
Nondimensional Axial Plane: −0.1290

Impeller Inlet Flow Coefficient:	0.144
Inducer:	ADP
Impeller:	Consortium Baseline
Avg. Test Speed:	6322 rpm
Arc Angle:	90 deg
Orientation Angle:	1.63 deg
Wall Avg. Static Head Coefficient:	0.1568
Continuity Match %:	98.64973

Overall Impeller Inlet Flow Characteristics

Radial Position	% Annulus	C/Utip avg.	Cu/Utip avg.	Ca/Utip avg.	Flow Ang. (deg)	W/Utip avg.	Wu/Utip avg.	Rel. Ang. (deg)
1	10	0.2424	0.2079	0.1242	30.86	0.2763	0.2468	26.72
2	15	0.2363	0.2015	0.1228	31.37	0.2919	0.2648	24.89
3	25	0.2257	0.1913	0.1193	31.94	0.3214	0.2985	21.78
4	35	0.2191	0.1876	0.1127	30.99	0.3445	0.3256	19.09
5	45	0.2173	0.1906	0.1039	28.59	0.3613	0.3460	16.71
6	55	0.2163	0.1946	0.0939	25.75	0.3774	0.3655	14.40
7	65	0.2235	0.2067	0.0840	22.10	0.3860	0.3768	12.56
8	75	0.2348	0.2220	0.0751	18.68	0.3922	0.3849	11.04
9	85	0.2405	0.2312	0.0655	15.82	0.4045	0.3992	9.32
10	95	0.2264	0.2195	0.0556	14.22	0.4379	0.4343	7.30

Bulk flow-weighted quantities across inlet annulus

Cu/Utip:	0.2038
Ca/Utip:	0.0928
Flow Angle from Tangential:	24.49
Wu/Utip:	0.3370
Relative Flow Angle:	15.40

Pump CFD Code Validation Tests
Axial = −0.1290 Imp. In Flow Coeff = 0.144

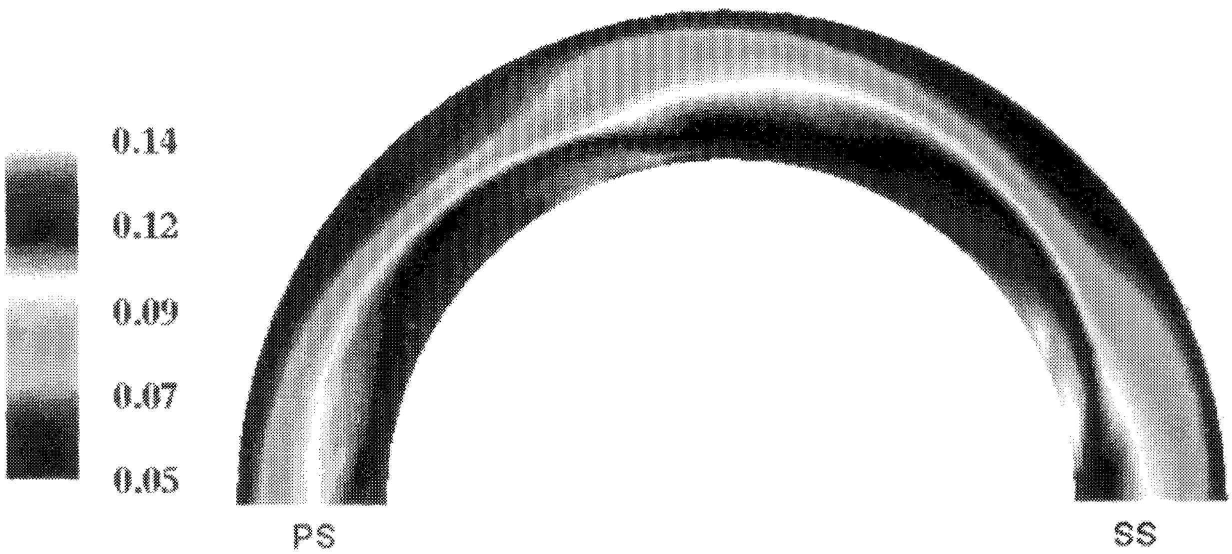

FIGURE 4 Consortium baseline impeller inlet laser survey (nondimensional axial velocity Ca). 6809-4

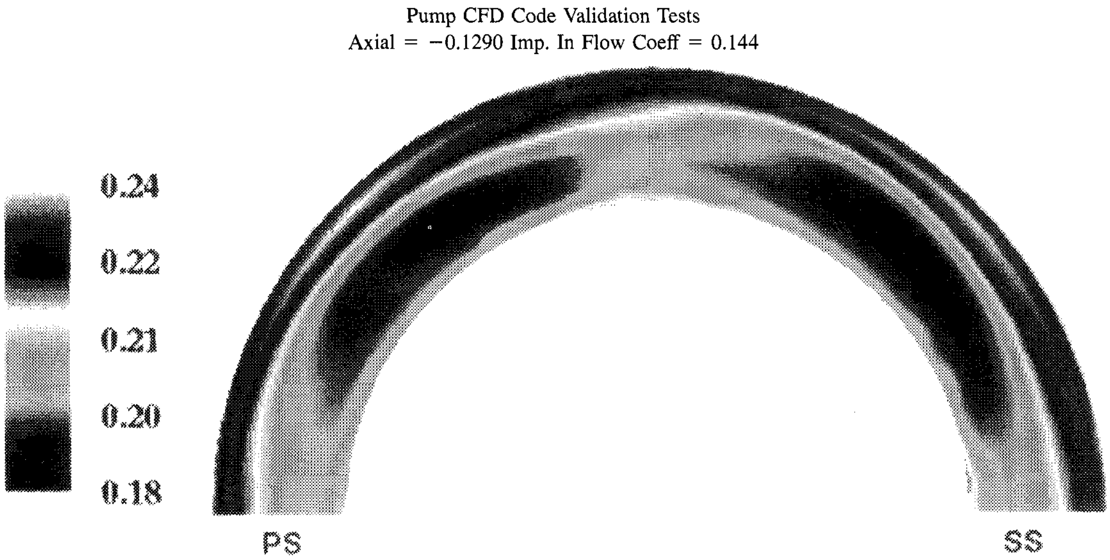

FIGURE 5 Consortium baseline impeller inlet laser survey (nondimensional tangential velocity Cu). 6809–5

TABLE 5
Impeller discharge flow characteristics

NRA Pump CFD Code Validation Test	
Laser Velocimeter surveys, ambient water, impeller discharge survey	
Test Number: t92a063-66,81	Test Date: November 1992
Nondimensional Radial Plane:	0.5138
Impeller Inlet Flow Coefficient:	0.144
Inducer:	ADP
Impeller:	Consortium Baseline
Avg. Test Speed:	6322 rpm
Arc Angle:	60 deg
Inlet Static Head Coefficient:	0.1530
Orientation Angle:	1.69 deg
Relative Angle:	31.724 deg
Wall Static Head Coefficient:	0.5196
Continuity Match % across B2:	115.2489
Overall Impeller Discharge Flow Characteristics	

Axial Position	% B2	C/Utip avg.	Cu/Utip avg.	Cr/Utip avg.	Flow Ang. (deg)	W/Utip avg.	Wu/Utip avg.	Rel. Flow (deg)
1	125.9	0.4887	0.4640	−0.1520	−18.14	0.5837	0.5635	15.09
2	106.7	0.4760	0.4751	−0.0250	−3.02	0.5530	0.5524	2.59
3	87.5	0.5342	0.5269	0.0693	7.49	0.5054	0.5006	7.88
4	75.0	0.6365	0.6289	0.0841	7.62	0.4074	0.3986	11.91
5	62.5	0.7112	0.7022	0.1073	8.69	0.3425	0.3253	18.25
6	50.0	0.7470	0.7351	0.1206	9.32	0.3163	0.2924	22.41
7	37.5	0.7154	0.7067	0.1049	8.44	0.3375	0.3208	18.10
8	25.0	0.6696	0.6613	0.0761	6.56	0.3740	0.3662	11.74
9	12.5	0.6374	0.6287	0.0623	5.66	0.4036	0.3988	8.88
10	−25.1	0.5661	0.5656	−0.0166	−1.68	0.4622	0.4619	2.06
11	−32.6	0.5679	0.5651	−0.0563	−5.69	0.4659	0.4625	6.93

Bulk flow-weighted quantities across discharge plane	
Cu/Utip:	0.8125
Cr/Utip:	0.0265
Flow Angle from Tangential:	1.87
Wu/Utp:	0.2151
Relative Flow Angle:	7.04

B_2 width, immediately downstream of the impeller, is 115.2%. A number greater than 100% is attributed to laser survey grid coarseness coupled with the trapezoid integration method used to calculate the flow rate. At the plane located further downstream, calculated flow deviated only by 1% from the measured flow. This excellent continuity match is attributed to obtaining data that on the average represented the overall flow characteristics of the discharge channel.

Tables 5 and 6 present summaries of the impeller discharge flow characteristics for the two radial planes. Figures 6 and 7 present contour plots of flow absolute radial velocity and absolute tangential velocity components at the impeller discharge. Each of the contour plots contains data for the two radial planes. The plane on the left side is nearest to the impeller discharge.

From the presented plots, the impeller discharge wakes are clearly evident in the plane immediately downstream of the impeller. Regions of low radial velocity, absolute flow angle, and high tangential velocity extend over most of the axial region, hub to shroud, in the wake defect areas. At a radial plane further downstream from the impeller, this becomes less distinct since mixing causes the flow to become more uniform. The nondimensional radial velocity clearly shows secondary flow downward into the impeller shroud and hub clearance.

A circumferential variation in impeller discharge static head coefficient of 1.1% was measured. This value is slightly outside the range of transducer accuracy. The majority of circumferential variation in impeller discharge static head coefficient may be attributed to trans-

TABLE 6
Impeller discharge flow characteristics

NRA Pump CFD Code Validation Test
Laser Velocimeter surveys, ambient water, impeller discharge survey

Test Number: t92a067-69,81	Test Date: October 1992
Nondimensional Radial Plane:	0.5596
Impeller Inlet Flow Coefficient:	0.144
Inducer:	ADP
Impeller:	Consortium Baseline
Avg. Test Speed:	6322 rpm
Arc Angle:	60 deg
Inlet Static Head Coefficient:	0.1530
Orientation Angle:	1.69 deg
Relative Angle:	31.67 deg
Wall Static Head Coefficient:	0.5460
Continuity Match %:	101.2291

Overall Impeller Discharge Flow Characteristics

Axial Position	% B2	C/Utip avg.	Cu/Utip avg.	Cr/Utip avg.	Flow Ang. (deg)	W/Utip avg.	Wu/Utip avg.	Rel. Flow (deg)
1	122.56	0.5158	0.5045	−0.1056	−11.82	0.6238	0.6148	9.75
2	102.95	0.5398	0.5395	−0.0167	−1.77	0.5801	0.5798	1.65
3	83.33	0.5483	0.5448	0.0598	6.26	0.5776	0.5745	5.94
4	66.67	0.5932	0.5792	0.1264	12.31	0.5547	0.5401	13.17
5	50.00	0.6356	0.6099	0.1754	16.05	0.5387	0.5094	19.00
6	33.33	0.6245	0.6043	0.1560	14.48	0.5381	0.5150	16.86
7	16.67	0.5848	0.5762	0.0970	9.56	0.5517	0.5431	10.13
8	−25.15	0.5580	0.5549	−0.0585	−6.02	0.5674	0.5644	5.92
9	−32.59	0.5562	0.5491	−0.0879	−9.10	0.5769	0.5702	8.77

Bulk flow-weighted quantities across discharge plane

Cu/Utip:	0.6259
Cr/Utip:	0.0409
Flow Angle from Tangential:	3.74
Wu/Utp:	0.4934
Relative Flow Angle:	4.73

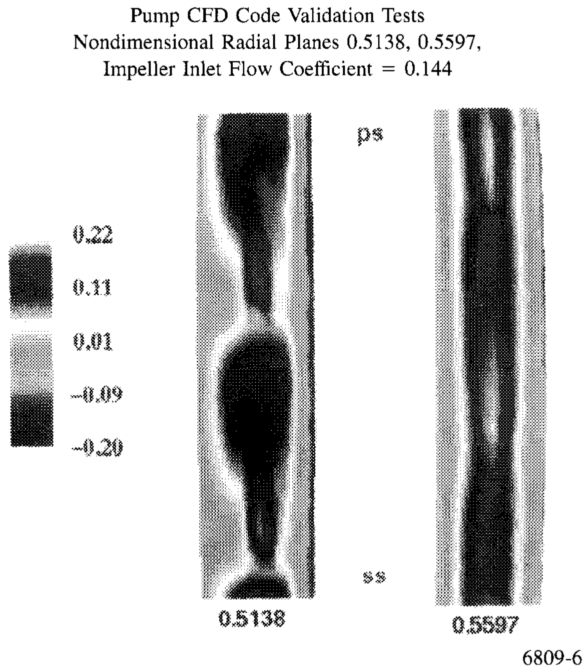

FIGURE 6 Consortium baseline impeller discharge laser survey (nondimensional radial velocity Cr).

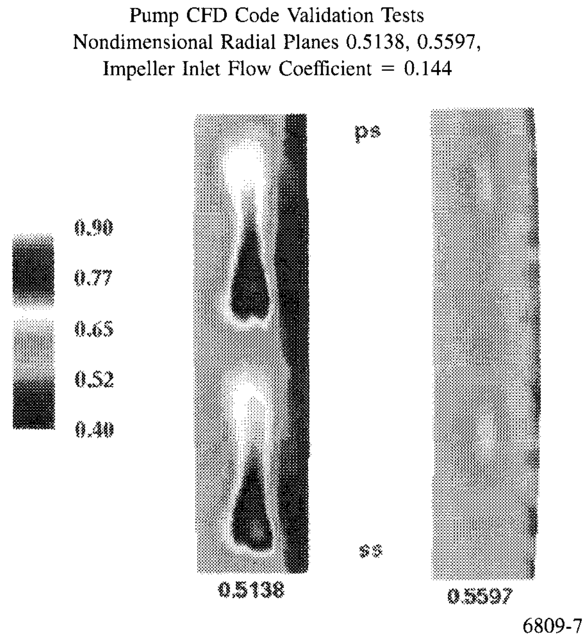

FIGURE 7 Consortium baseline impeller discharge laser survey (nondimensional tangential velocity Cu).

ducer accuracy with a slight contribution caused by an asymmetric discharge flow condition. The crossover discharge was effective in eliminating the typical discharge flow asymmetry.

The impeller discharge laser survey traversed the impeller discharge channel while commencing in the same location circumferentially for each axial location. No attempt was made to alter the circumferential start location to coincide with the impeller full blade; thus, a rectangular grid results. A calculation was performed that defined which data windows corresponded to the individual flow passages in the plane immediately downstream of the impeller. In this manner a flow split among the two blade passages encompassed by the laser survey was performed. The passage between the first full blade and the partial blade was calculated to contain 49% of the total flow. The percent of calculated flow in the passage between the partial blade and the adjacent full blade was 51% of total flow. This type of uneven flow distribution, driven by secondary flow along the suction surface, was similarly exhibited in Reference [1].

CONCLUSION

A test program to obtain benchmark quality data for typical rocket engine pump geometry was successfully performed in Rocketdyne's EDL PTF. Data were obtained nonintrusively with a L2F velocimeter, static pressures were included at key locations to provide boundary conditions for CFD code validation. Laser surveys at the inlet and discharge of a Rocketdyne-designed impeller were performed. Repeatability of test conditions was demonstrated over the entire test duration.

The success of this empirical study adds significantly to the limited database of accurate centrifugal impeller flow field measurements. Further laser velocimeter surveys throughout various pump components will permit additional CFD code benchmarking data to be acquired and, ultimately, to a better understanding of fluid phenomena.

Nomenclature

B_2	impeller passage discharge width
C	absolute velocity
Ca	absolute axial velocity component
C_r	absolute radial velocity component
C_t	absolute tangential velocity component
C_u	absolute tangential velocity component
U_{tip}	impeller tip tangential velocity

Acknowledgments

The authors would like to acknowledge NASA-MSFC, with technical monitor Mr. Roberto Garcia, for funding the empirical study; Rocketdyne's Engineering Development Laboratory personnel, James J. Lesch, William L. Lowe, and Robert D. McGlynn for contributing to the success of the project and Michael R. Yandell for his design contributions and support during fabrication.

References

Brozowski, L. A., Ferguson, T. V., Lee, G. A., Prueger, G. H., and Rojas, L., "Laser Velocimeter Measurements of an Impeller Flow Field," ASME Fluids Engineering Conference Second Pumping Machinery Symposium, June 1993a, Washington D.C., Vol. 154, pp. 187–196.

Brozowski, L. A., Ferguson, T. V., and Rojas, L., "Impeller Flow Field Characterization With a Laser Two-Focus Velocimeter," presented at the 11th Workshop for Computational Fluid Dynamics Applications in Rocket Propulsion, 20–22 April 1993b, Marshall Space Flight Center, Alabama.

Garcia, R., Jackson, E. D., and Schutzenhofer, L. A., "A Summary of the Activities of the NASA/MSFC Pump Stage Technology Team," 4th ISROMAC, April 1992, pp. 88–96.